https://dx.doi.org/10.1016/j.compgeo.2017.05.015

This is the Pre-Published Version.

Experimental and theoretical investigation on the compression behavior of sand-marine clay mixtures within homogenization framework

by

Xiusong Shi
Department of Civil and Environmental Engineering,
The Hong Kong Polytechnic University, Hung Hom, Kowloon, Hong Kong.
Email: xsshi@polyu.edu.hk

and

Jianhua YIN
Department of Civil and Environmental Engineering
The Hong Kong Polytechnic University, Hung Hom, Kowloon, Hong Kong, China
Tel: (852) 2766-6065, Fax: (852) 2334-6389, Email: cejhyin@polyu.edu.hk

March 2017

© 2017. This manuscript version is made available under the CC-BY-NC-ND 4.0 license http://creativecommons.org/licenses/by-nc-nd/4.0/

Abstract:

In land reclamation or soil improvement projects, the layered sand-clay scheme is usually used to accelerate the consolidation process. However, sand particles may percolate into the soft clay layer at the sand-clay interface. The behavior of the mixed soil in vicinity of the sand-clay interface affects the deformation of the underneath clay layer. In this paper, the compression behavior of sand-marine clay mixtures was investigated, both experimentally and theoretically. The test data reveal that the Normal Compression Line of a sand-clay mixture depends on both the sand fraction and the initial water content of the clay matrix. The local stress in the clay matrix σ'_C is approximately close to the overall stress of the sand-clay mixture σ' for a sand mass fraction of 20%. The stress ratio, σ'_C/σ', falls significantly with increasing overall stress for a sand fraction of 60%, which may be attributed to the formation of clay bridges between adjacent sand particles. A compression model was formulated within the homogenization framework. First, a homogenization equation was proposed, which gives a relationship between the overall stiffness E and that of the clay matrix E_C. Then, a model parameter ξ was incorporated considering the sensitivity of the structure parameter on the volume fraction of the clay matrix. Finally, a simple compression model with three model parameters was formulated using the tangent stiffness. Comparisons between the experimental data and simulations reveal that the proposed model can well represent the compression curves of the sand-marine clay mixtures observed in the laboratory.

Keywords: Marine clay; Sand-clay mixtures; Compressibility; Homogenization; Tangent stiffness

1 Introduction

Natural soils are usually composite soils consisting of coarse particles and fine materials filling the inter-granular space (Yin, 1999; Chu and Leong, 2002; Monkul and Ozden, 2007; Watabe, *et al.*, 2011). Similar composite materials are also being produced by human activities, e.g., land reclamation (Karunaratne *et al*., 1990, 1991; Tan *et al*., 1994), soft soil improvement project (Silva, 2016), and inland waste disposal facilities (Graham, *et al.*1989). The compression of these composite soils has been a matter of concern. To this end, the compression behavior of a sand-marine clay mixture is investigated in this paper in order to better understand the mechanisms governing the overall compression behavior, and to proposed a simple model for binary sand-clay mixtures.

The compression behavior of sand-clay mixtures was well documented by many researchers before. Most of them focused on the effect of fine materials on the overall compressibility. Yin (1999) did a series of oedometer tests on the Hong Kong marine deposits, and obtained correlations between the compression index and plasticity index and clay content. Similar works were done by Fukue *et al*., (1986), Graham *et al*., (1989); Martins *et al*., (2001) and Elkady *et al*., (2015). Further investigations were put forward by considering the clay-sand interplay with different clay fractions (Pitman *et al*., 1994; Kumar, 1996; Kumar and Wood, 1999; Boutin *et al*., 2001; Chu and Leong, 2002; Monkul *et al*., 2005, 2006; Chu *et al*., 2017). It was postulated that the mixtures would behave as that of the soft clay matrix when the volume fraction of fine material approached a certain value (denoted as 'transition fine content') which varies with the shape, particle size distribution of the coarse inclusions. Some researchers denoted that the formation of skeleton was also affected by the stress level (Monkul and Ozden, 2007), since the volume of inter-granular material decreases with increasing stress.

In most of the previous literature, it was assumed that the Normal Compression Line

(NCL) of a clay matrix was unique. Hence, only the influence of mass fraction was investigated. In Yin's work (Yin, 1999), the overall initial water content of the samples (sand-clay mixtures with different mass fractions of sand) is close to the corresponding liquid limit. In this case, the initial water content of the clay matrix in the mixtures may not be the same. Recent publications revealed that the NCL of a clay is not unique, which is affected by the initial water content (Cerato and Lutenegger, 2004; Hong *et al*., 2010; Liu *et al*., 2013; Shi and Herle, 2015; Tsuchida, 2017; Zeng *et al*., 2015; Horpibulsuk *et al*., 2016; Zeng *et al*., 2016a and 2016b). Consequently, the compression curves of sand-clay mixtures with different initial water contents of the clay matrix are not comparable.

Sand-clay mixtures with different sand fractions and different initial water contents of the matrix are investigated in this paper. Afterwards, a simple compression model is proposed within the homogenization framework and is validated by the test results.

2 Volume groups and definitions of sand-clay mixtures

2.1 Volume groups of sand-clay mixtures

The volume groups of a sand-clay matrix shall be clarified first. Afterwards, definitions of homogenized variables are given. A sand-clay mixture consists of a clay matrix ("clay" here includes both clay minerals and silts) and solids of sand (Fig. 1). As a first approximation, it is assumed that the sand particles are incompressible and do not have water-holding capacity (Mitchell, 1993; Monkul and Ozden, 2007), i.e., the stiffness of sand is far higher than that of the clay matrix, and the water in a sand-clay mixture is only associated with the clay matrix. In this case, the volume fraction of the clay matrix decreases with increasing stress level.

The marine clay used in this study contains silts and clay minerals. Hence, after being mixed with coarse sands, the resulting mixture consists of sands, silts, and clay minerals (see Fig. 1). A Representative Elementary Volume (REV) of a sand-clay mixture is divided into three volume groups: the voids in the clay matrix V_V, including the inter-aggregate pores and intra-aggregate pores (Mitchell, 1993); the volume occupied by solids in the clay matrix V_{SC}, consisting of the silts and clay particles, and the volume of sand particles V_{SS}.

Two levels of porosity are defined: the porosity of the clay matrix n_C and the overall porosity n (porosity of the sand-clay mixtures). They are defined as

$$n_c = \frac{V_v}{V_v + V_{sc}}; \quad n = \frac{V_v}{V_v + V_{sc} + V_{ss}} \tag{1}$$

Correspondingly, two void ratios, the void ratio of the clay matrix e_c and the overall void ratio e, are defined as

$$e_c = \frac{V_v}{V_{sc}}; \quad e = \frac{V_v}{V_{sc} + V_{ss}} \tag{2}$$

From the above definitions, the local porosity n_c is related to its corresponding overall value using the volume fraction of the clay matrix ϕ_c:

$$n = \phi_c n_c \tag{3}$$

ϕ_c is defined as

$$\phi_c = \frac{V_{tc}}{V_{tc} + V_{ss}} \tag{4}$$

where $V_{tc} = V_{sc} + V_v$ is the total volume of the clay matrix. ϕ_c can be derived from Eq. (3), which is expressed in terms of the overall porosity and the porosity of the clay matrix as

$$\phi_c = \frac{n}{n_c} \tag{5}$$

As discussed above, ϕ_c is a stress dependent variable. Eq. (5) will be used later to update the volume fraction of the clay matrix with increasing stress level. Both n and n_c are related to the corresponding void ratios:

$$n = \frac{e}{1+e}; \quad n_c = \frac{e_c}{1+e_c} \tag{6}$$

In model predictions, the void ratios can be calculated from the current strains[1] and the initial void ratios:

$$e = (1 + e_0)\exp(-\varepsilon) - 1; \quad e_c = (1 + e_{c0})\exp(-\varepsilon_c) - 1 \tag{7}$$

where e_{c0} and e_0 are the corresponding initial void ratios, and ε_c and ε are the current vertical strains of the clay matrix and its corresponding overall value, respectively. Their definitions will be provided in the next subsection.

2.2 Definition of stresses and strains

The presence of stiff sand particles increases the stiffness of a sand-clay mixture, since the local stress $\boldsymbol{\sigma}'(\boldsymbol{x})$ and strain $\boldsymbol{\varepsilon}(\boldsymbol{x})$ fields are not uniform on the micro-scale (Tandon and Weng, 1988; Kumar, 1996). The average stress in the composite is higher than that in the matrix, whereas, the strain is reduced compared with the matrix. The solution of the stress (strain) field is a tricky problem which can be simplified by considering volume-average stress and strain in each phase. Given a representative volume V_t (Fig. 1), the overall stress σ' and strain ε can be defined as the average of the local stress $\boldsymbol{\sigma}'(\boldsymbol{x})$ and the local strain $\boldsymbol{\varepsilon}(\boldsymbol{x})$ over the total representative volume:

$$\sigma' = \frac{1}{V_t}\int_{V_t} \boldsymbol{\sigma}'(\boldsymbol{x})\mathrm{d}V; \quad \varepsilon = \frac{1}{V_t}\int_{V_t} \boldsymbol{\varepsilon}(\boldsymbol{x})\mathrm{d}V \tag{8}$$

Analogously, the volume-average stress and strain of the constituents (sands and soft clay

[1] Since the samples have a large deformation at high stress levels during oedometer compression tests, the logarithmic strain is used for in this paper.

matrix, respectively) can be defined over the corresponding volumes[2]:

$$\sigma'_c = \frac{1}{V_{tc}} \int_{V_{tc}} \boldsymbol{\sigma}'(\boldsymbol{x}) \mathrm{d}V; \quad \sigma'_s = \frac{1}{V_{ss}} \int_{V_{ss}} \boldsymbol{\sigma}'(\boldsymbol{x}) \mathrm{d}V; \quad \varepsilon_c = \frac{1}{V_{tc}} \int_{V_{tc}} \boldsymbol{\varepsilon}(\boldsymbol{x}) \mathrm{d}V \tag{9}$$

where σ'_c (ε_c) and σ'_s are the volume-average stresses (strain) in the clay matrix and sand, respectively. Combining Eqs (8) and (9), and considering the definition of the volume groups, one obtains the relationship between the overall volume-average stress (strain) and those of its constituents:

$$\sigma' = \frac{1}{V_t} \int_{V_t} \boldsymbol{\sigma}'(\boldsymbol{x}) \mathrm{d}V = \frac{1}{V_t} \int_{V_{tc}} \boldsymbol{\sigma}'(\boldsymbol{x}) \mathrm{d}V + \frac{1}{V_t} \int_{V_{ss}} \boldsymbol{\sigma}'(\boldsymbol{x}) \mathrm{d}V = \phi_c \sigma'_c + (1 - \phi_c) \sigma'_s \tag{10a}$$

$$\varepsilon = \frac{1}{V_t} \int_{V_t} \boldsymbol{\varepsilon}(\boldsymbol{x}) \mathrm{d}V = \frac{1}{V_t} \int_{V_{tc}} \boldsymbol{\varepsilon}(\boldsymbol{x}) \mathrm{d}V = \phi_c \varepsilon_c \tag{10b}$$

Given the definition of variables (stresses, strains, void ratios and porosities), the test data can be analyzed within the homogenization framework.

3 Materials and test program

The materials used in this study are a marine clay and a coarse sand material from Hong Kong. The basic physical properties of the materials (according to British Standard 1377) are given in Table 1. To investigate the inter-granular structure effect of the sand-clay mixture, only the sand particles with an essentially uniform grading between 1.0 *mm* and 2.0 *mm* were used in this study. The shape of sand particles ranged from subangular to angular with the maximum void ratio (e_{smax}) of 0.945 and the minimum void ratio (e_{smin}) of 0.601, respectively, which are similar to those of Hostun RF sand (Saada and Puccini, 1988) and Toyoura sand (Fukushima and Tatsuoka, 1984).

[2] The sand particles are assumed to be incompressible, hence, the corresponding strain is not considered.

The original clay was first mixed with water and then sieved with a mesh opening of 0.063 *mm* to exclude coarse grains from the natural marine soil. In this case, all the coarse particles in the sand-clay mixtures are from the coarse sand material. Due to the high initial water content of the clay slurry, the soil was exposed to air for a period of time. When the water content was reduced to its liquid limit, the sample was poured into four individual containers. Afterwards, water was added to reach the desired water contents: $1.09w_L$, $1.19w_L$, $1.39w_L$ and $1.60w_L$, respectively. For the production of a sand-clay mixture, the mass of the sand inclusions m_S was calculated according to the initial water content of the clay matrix w_c and its expected proportion in the mixture:

$$m_s = \frac{(1 - \psi_c)m_c}{\psi_c(1 + w_c)} \tag{11}$$

where ψ_c is the dry mass fraction of the clay matrix in the sand-clay mixture (four different dry clay mass fractions: 100%, 80%, 60%, 40% were considered in this study), and m_C is the mass of the clay matrix. The sand particles and the clay slurry were mixed homogeneously and then spooned into a container. To expel possibly trapped air bubbles in the sample, a vibration process was further applied by hitting the container on a table. Since the vibration process may lead to a non-uniform distribution of the sand particles in the mixture, the samples were mixed carefully to make it homogeneously. The samples were then kept in an airtight container for 3 days for a complete saturation. Afterwards, the sand-clay mixtures were spooned into the consolidation rings (with a diameter of 70.0 mm and a height of 19.0 mm) by a palette knife. After testing, the samples were dried in the oven for 24 h, and the theoretically initial water content was estimated from the dry masses and the initial size of the samples by considering a fully saturated condition. All the specimens investigated have a saturation ratio (between the measured initial water content and the corresponding theoretically value) higher than 0.98.

In order to avoid soil squeezing between the consolidation ring and the loading cap, specimens were consolidated at an initial vertical stress of 1.7 kPa. The consolidation stress was then gradually increased following steps of 2.5, 5, 10, 25, 50, 100, 200, 400, 800 and 1200 kPa. The duration of every load increment was 8-24 h in order to dissipate excess pore pressures according to the corresponding consolidation curves.

4 Test results and analysis

To calculate the void ratio of a mixture, the overall particle density should be determined. In some previous work, the specific gravity of mixtures was calculated by the weighted average method which is only a rough estimation. Actually, the overall particle density can be determined by the particle density of its constituents using

$$\rho = \frac{\rho_c \rho_s}{\psi_c \rho_s + (1 - \psi_c)\rho_c} \tag{12}$$

The results of compression tests on the sand-clay mixtures (samples with a given initial water content and different mass fractions) are shown in Fig. 2 in terms of overall specific volume (v = 1+ e) and overall effective vertical stress on a semi-logarithmic scale. It is seen that the compression curves show an approximately linear relationship at a lower initial water content of the clay matrix (1.09 w_L), which becomes slightly concave upwards with increasing initial water content of the matrix. Additionally, the compressibility decreases with the increase of sand volume fraction.

To clearly show the effect of initial water content on the overall compression behavior of the clay mixtures (or the pure clay), the results of samples with a given mass fraction are shown in Fig. 3 on a semi-logarithmic scale. It can be seen that the curve for a higher initial water content of the pure clay lies above that for a lower one, and the corresponding compressibility increases with increasing initial water content. It indicates that the Normal Compression Line of the investigated clay is not unique, which is significantly affected by the initial water content. Correspondingly, the compression curves of the mixtures show similar pattern (with the pure clay) that the initial water content has an influence on the overall compression behavior. However, the decrease of compressibility is not as distinct as that of the pure clay, since it was reduced due to the increase volume fraction of the (incompressible) sand particles.

The compression curves of sand-clay mixtures (or the pure clay) (Fig. 2) show similar pattern as those of natural soils, especially for those with a lower initial water content of the clay matrix (e.g., 1.09 w_L and 1.19 w_L). The overall stiffness shows a sharp change in the vicinity of a stress level, which is named as the remolded yield stress σ'_y (Hong *et al.*, 2012). The curves with a slightly inverse ’S’ shape on the semi-logarithmic scale can be well represented by a straight line beyond the remolded yield stress in the double logarithmic plot as described in Fig. 4.

$$\ln v = N - \lambda \ln(\sigma'/\sigma'_r) \tag{13a}$$

$$\ln v_c = N_c - \lambda_c \ln(\sigma'_c/\sigma'_r) \tag{13b}$$

where σ'_r =1 kPa is a reference stress, N and λ are compression parameters for the sand-clay mixtures, N_c and λ_c are the compression parameters for pure clay matrix (N and N_c corresponding to the reference stress, and λ and λ_c being the slope of the Normal Compression Line in double logarithmic plot). The above equation was proposed by Butterfield (1979) and Hashiguchi (1995) for natural soils, which was verified by many researchers for remolded soils (e.g., Sridharan and Prakash, 1996; Hong and Onitsuka, 1998; Hong *et al.*, 2010; Shi and Herle, 2015, 2016b) beyond the remolded yield stress. The remolded yield stress is linked to the suction pressure on the surface of the specimen during the air drying and preparation process (Fredlund, 1964), which increases with decrease of the initial water content for a given soil (Hong, 2007; Hong *et al.*, 2010; Shi and Herle, 2015). Due to absence of compression data within very small stress levels, the remolded yield stress in this study was estimated by extrapolating the post-yield curve to the initial void ratio (Hong, 2007). It is seen from Fig. 5 that it decreases with increasing initial water content of the clay matrix, but it is not sensitive to the sand fraction. In the sequel, only the data beyond the remolded yield stress are analyzed. Hence, the model is not suitable for the stress smaller than the remolded yield stress of sand-clay mixtures.

The intrinsic compression void e^*_{100} (void ratio at a stress of 100 kPa) and compression index C^*_c (difference of the void ratio between 100 kPa and 1000 kPa) can be calculated using Eq. (13a) and (13b) which was fitted with the data beyond the remolded yield stress. The results in Fig. 6 indicate that both compression parameters increase with the mass fraction and the initial water content of the clay matrix. The difference of compression parameters with different initial water contents is significant for a given mass fraction of 100% (pure clay), which reduces as the initial water content falls. This confirms the point that the Normal Compression Line (both the pure clay and the sand-clay mixtures) varies with the initial water content, indicating that the only the mixtures with the same initial water content of the clay matrix are comparable.

The intrinsic void index $I_v = (1 - e^*_{100})/C^*_c$ was introduced by Burland (1990) for correlating the compression curves of remolded clays by moving them to a fixed point (I_V= 0 at σ'=100 kPa):

$$I_v = 2.45 - 1.285\log\sigma' + 0.015(\log\sigma')^3 \quad (14)$$

The oedometer data are plotted in Fig. 7 in terms of void index and effective vertical stress. The compression curves can be normalized using the intrinsic compression parameters (e^*_{100} and C^*_c) beyond 5 kPa within the testing stress range. Some differences arise at very small stress levels due to the remolded yield stress, especially for the samples with lower initial water content of the clay matrix.

5 Homogenization equation

5.1 Local stress distribution

Considering that the sand particles are incompressible compared with the clay matrix within the testing stress range, and that the water in the mixtures are only associated with the clay matrix, the void ratio of the clay matrix is given as

$$e_c = \frac{e\rho_c}{\psi_c \rho} \tag{15}$$

Substitution of Eqs (12) and (13a) into Eq. (15), one gets the local void ratio e_c at a given overall stress. Fig. 8 shows the relationship between the local specific volume (v_c = 1+e_c) and the overall effective vertical stress. It is seen that the curves with a sand fraction of 20% are approximately close to those of the corresponding pure clay samples. The data points move upwards as the sand fraction and the effective vertical stress increase, indicating that the stress distribution is not uniform. Assuming that the compression curve of the matrix in a sand-clay mixture follows the Normal Compression Line of the pure clay at a specified initial water content regardless of the sand fractions, the volume average stress in the clay matrix σ'_c can be estimated (see Fig. 9). At a given overall stress level, the specific volume of the clay matrix is computed using Eqs (13b) and (15). Then, the local stress in the clay matrix is calculated as

$$\sigma_c' = \exp\left(\frac{N_c - \ln v_c}{\lambda_c}\right)\sigma_r' \tag{16}$$

where N_c and λ_c are intrinsic compression parameters corresponding to the pure clay. Two points need to be clarified when using Eq. (16): (1) the initial water content of the clay matrix in a clay mixture should be consistent with that of the corresponding pure clay; (2) it is only applicable to the stress levels beyond the remolded yield stress of the clay matrix. To describe the stress distribution in a mixture, a stress ratio is defined as the ratio between the stress of the clay matrix and the overall value. The evolution of the stress ratio σ_c'/σ' of the mixtures is shown in Fig. 10. It is clear that the stress ratio of the mixtures is close to one for a sand mass fraction of 20%, since the compression curves nearly overlap those of the pure clay. In addition, the stress ratio decreases with the mass fraction of sand particles; however, there is no obvious change of the stress ratio with the increase of the initial water content of the clay matrix.

The stress ratio falls significantly for a sand fraction of 60% as the effective vertical stress increases, which tends to suggest that the sand particles are approaching each other. To investigate the evolution of the inter-granular structure (sand particles), the volume fraction of the clay matrix needs to be analyzed. It can be computed from Eqs (5), (6) and (15).

Data of the volume fraction of the clay matrix (different dry mass fractions and different initial water contents of the clay matrix) are gathered in Fig. 11. ϕ_c falls with increasing overall effective vertical stress. The horizontal line gives a constant value (ϕ_c = 0.486) of the volume fraction of the clay matrix, named as 'transition fines content ϕ_{ct}' after Monkul and Ozden (2005). It corresponds to the maximum void ratio of the sand material (e_{smax} = 0.945). Recalling that the stress ratio decreases significantly with increasing stress level for a sand fraction of 60%, however, the volume fraction still lies above the transition fines content. One possible explanation is that a part of the clay matrix acts like bridges between adjacent coarse particles, which contributes to the overall force chain (Jafari and Shafiee, 2004). Consequently, the corresponding stress ratio decreases.

5.2 A homogenization equation

A sand-clay mixture is a random particulate composite (Hashin, 1983), characterized by some degree of disorder on a local scale (Fig. 1). A similar composite material, named as 'lumpy-composite soil' consisting of deformable clayey lumps and a reconstituted soil, was investigated by Shi and Herle (2016a). Theoretical and numerical analysis revealed that the logarithm of the overall stiffness could be computed as a volume average value of the ones of its constituents. However, the overall stiffness of sand-clay mixtures would be significantly overestimated using this homogenization approach (Shi and Herle, 2016a), since the sand particles are incompressible ($E_S = \infty$).

One possible postulation is that the overall stiffness depends on the reconstituted clay matrix regardless of the inclusions. Tu *et al.* 's investigation (Tu *et al.*, 2005) on a random particulate composite (both the matrix and inclusions are ideal elastic materials, with elastic stiffness of E_m and E_i, respectively) suggested that improving the elastic stiffness of inclusions significantly enhanced the overall elastic stiffness E at first but it comes to a limit state and cannot be further increased after approaching a transition point. Hashin (1983) pointed out that when a soft matrix was reinforced by rigid lumps (corresponding to sand-clay mixtures in this study), the stiffness of the composite can only increase to several times the matrix stiffness, which corresponds to a limit state in Fig. 12. In this case, a homogenization equation coupling the overall stiffness E and that of the clay matrix E_c needs to be investigated.

A homogenization equation can be proposed based on either secant or tangent stiffness. The latter one is adopted in this study, since tangent formulations are widely used in soil mechanics. The overall tangent stiffness of the mixtures was computed from two neighboring data points in the compression plots, and the tangent stiffness of the clay matrix can be deduced from Eq. (16):

$$E_c = \frac{\mathrm{d}\sigma_c'}{\mathrm{d}\varepsilon_c} = \frac{\mathrm{d}\sigma_c'}{\mathrm{d}(\ln v_{c0} - \ln v_c)} = \frac{\sigma_c'}{\lambda_c} \tag{17}$$

where $v_{c0} = 1 + e_0$ is the initial specific volume of the clay matrix. Fig. 13 shows the relationship between the overall tangent stiffness and that of the matrix (overall effective stress higher than 10 kPa). It can be seen that the mass fraction of the clay matrix significantly affects the homogenization relationship; however, data with different mass fractions can be well extrapolated to the origin in the double-logarithmic plot (E=1 and E_c=1). Hence, a possible homogenization equation can be given as

$$\ln E = \chi \phi_c \ln E_c \tag{18}$$

where χ is a structure variable parameter governing the structure transition of the inter-granular structure of sand-clay mixtures. It is calculated from Eqs (17) and (18) at given stress levels, as shown in Fig.14. The data show a relatively consistent relationship: it increases slightly with increasing stress level and falls remarkably as the mass fraction of the clay matrix increases. After being presented as a plot of χ against the corresponding volume fraction of the clay matrix, an approximately unique relationship exists (Fig. 15). An expression for the structure variable should satisfy the following two requirements:

(1) The structure variable is approximately close to one if the volume fraction of sand inclusions is negligible. I.e., $\chi = 1$, when $\phi_c = 1$.

(2) The structure variable increases with decreasing volume fraction of the clay matrix, becomes infinite when approaching the minimum clay fraction which corresponds to the minimum void ratio of the sand material

The minimum void ratio of a pure sand material decreases with increasing stress level (Herle and Gudehus, 1999). A major factor is the fracturing and splitting of the sand particles (Pestana and Whittle, 1995; Mesri and Vardhanabhuti, 2009)). However, the breakage and induced rearrangement of sand particles in sand-clay mixtures could be substantially reduced due to the clay matrix within the inter-granular space: (1) the stress in a single sand particle is more uniform due to the confining stress from surrounding clay matrix, which prevents the fracturing and splitting of the sand particles; (2) since the degree of freedom of sand particles in the mixture is lower than that of the pure sand specimen, the rearrangement of the inter-granular is not so distinct. Consequently, the minimum inter-lump porosity for a binary sand-clay mixture is not sensitive to the stress level, and it can be approximated by the measured value according to the densification standard: BS1377 (e_{smin}=0.601).

After contacting each other, solid force chains form and the sand inclusions behave as a porous rock material. In this case, the sand structure would overtake a further load increment alone, $\chi = \infty$.

Considering the above requirements, a relationship between the structure variable and the volume fraction of the clay matrix is given as

$$\chi = \left(\frac{1 - \phi_{cmin}}{\phi_c - \phi_{cmin}} \right)^{\xi} \tag{19}$$

where ξ is a model parameter controlling the sensitivity of the structure variable on the volume fraction of the clay matrix (χ increases with increasing ξ for a given volume fraction of the clay matrix), ϕ_{cmin} is the minimum volume fraction of the clay matrix corresponding to the minimum void ratio of the sand material:

$$\phi_{cmin} = \frac{e_{smin}}{1 + e_{smin}} \tag{20}$$

As shown in Fig. 15, with $\xi = 0.75$, the test data can be well fitted. Note that the inter-granular porosity for a sand-clay mixture may be slightly lower than the ϕ_{cmin} in an extremely high stress level or very low initial inter-granular porosity. In this case, ϕ_{cmin} can be replaced by a value slightly lower than the minimum value to avoid irrational values of the structure variable. However, ϕ_{cmin} used in this study can well reproduce the compression data of the mixtures within the range of initial water content and sand fractions.

6 Compression model and its validation

6.1 A simple compression model

The compression behavior of an inhomogeneous material can be derived from two following relationships: (1) a homogenization equation relating the overall stiffness to those of its constituents. In case of sand-clay mixtures, the overall stiffness only depends on the clay matrix (Eq. (18)). (2) stress strain relationships of the constituents. Since the sand particles are assumed to be incompressible, only the incremental stress strain relationship of the clay matrix is considered (Eq. (17)).

From the homogenization equation (Eq. (18)) and the definition of the tangent stiffness, the tangent stiffness of sand-clay mixtures can now be deduced as

$$\frac{d\sigma'}{d\varepsilon} = \left(\frac{d\sigma'_c}{d\varepsilon_c}\right)^{\chi\phi_c} = \left(\frac{\sigma'_c}{\lambda_c}\right)^{\chi\phi_c} \tag{21}$$

χ and ϕ_c are state variables depending on the current void ratio of the clay matrix. The overall stiffness can be expressed as a function of a stress concentration ratio and the corresponding local stiffness (e.g., stiffness of the clay matrix), which was first proposed by Hill (1963). Considering the stress (strain) definitions (Eqs (8) - (10b)), the tangent stress strain relationship (Eq. (17)) and the homogenization equation (Eq. (18)), an incremental stress ratio μ_σ^c is deduced as

$$\mu_\sigma^c = \frac{\mathrm{d}\sigma'_c}{\mathrm{d}\sigma'} = \phi_c^{-1}\left(\frac{\sigma'_c}{\lambda_c}\right)^{1-\chi\phi_c} \tag{22}$$

Eqs (5) - (7), (17), (19), (21) and (22) present a full model for sand-clay mixtures. Eqs (5) - (7) determine the evolution of the volume fraction of the clay matrix; The structure parameter χ governing the homogenization relationship is given by Eq (19); The local stress increment in the clay matrix at a particular calculation step is obtained from Eq (22); The overall strain increment and the one of the clay matrix are computed from Eqs (17) and (21), respectively.

The compression model proposed in this paper is within the homogenization framework. The overall volume change equals that of the clay matrix, and the local stress in the clay matrix is governed by the inter-granular structure evolution. The modelling concept is different from that for structured soils (e.g., Cotecchia and Chandler, 2000; Masin, 2007; Liu *et al*., 2010). For a given sand fraction, there is no so called 'reference state' in a sand-clay mixture in 1D compression loading, and the structure variable coupling the overall stiffness and the local stiffness increases monotonically with increasing overall stress level.

6.2 Model parameters and numerical procedures

As can be seen from Eqs (5) - (7), (17), (19), (21) and (22), there are three model parameters for a given initial water content of the clay matrix: N_c, λ_c and ξ. N_c and λ_c are intrinsic model parameters describing the Normal Compression Line of the clay matrix at a given initial water content. ξ is a model parameter governing the evolution of internal structure of a sand-clay mixture. Note that N_c and λ_c vary with the initial water content of the clay matrix, which can be given by very simple equations (Shi and Herle, 2016b). For simplicity, in this work, the model parameters are fitted from the corresponding compression curves of the pure clay at different initial water contents (Table 2).

The compression curves of clay mixtures can be predicted with the following procedures:

Step 1. Determine an initial state of a clay mixture. Since the parameters in Table 2 describe only the Normal Compression Line of the clay matrix, a testing stress state σ'_0 beyond (or approximately close to) the remolded yield stress is used. For the sand-clay mixtures in this study, the initial stresses are given in Table 2.

Step 2. Compute the local stresses σ'_c and σ'_s at the designated initial state of a sand-clay mixture. Substitution of Eq. (15) into Eq. (16) and considering Eq. (10a), one gets the local stresses.

Step 3. Let $(\sigma')^{k-1}$ and ε^{k-1} represent the overall stress and strain at the last increment step. Similarly, $(\sigma'_c)^{k-1}$ and $(\varepsilon_c)^{k-1}$ denote the stress and strain in the clay matrix. The incremental stress ratio of the clay matrix is calculated according to Eq. (22).

Step 4. Given an overall stress increment $\mathrm{d}\sigma'$, compute the stress increment in the clay matrix: $\mathrm{d}\sigma'_c = \mu_\sigma^c \mathrm{d}\sigma'$. The current stress is updated: $(\sigma'_c)^k = (\sigma'_c)^{k-1} + \mathrm{d}\sigma'_c$; $(\sigma')^k = (\sigma')^{k-1} + \mathrm{d}\sigma'$.

Step 5. Calculate the overall strain increment $\mathrm{d}\varepsilon$ and that of the clay matrix $\mathrm{d}\varepsilon_c$ from Eqs (21) and (17), respectively. The current strains are updated: $(\varepsilon_c)^k = (\varepsilon_c)^{k-1} + \mathrm{d}\varepsilon_c$; $\varepsilon^k = \varepsilon^{k-1} + \mathrm{d}\varepsilon$.

Step 6. The volume fraction of the reconstituted soil should be updated using Eqs (5) - (7) at the end of every incremental step.

Step 7. The current structure parameter χ was computed from the volume fraction of the current clay matrix (Eq. (19)). Refer to Step 3 to continue for the next incremental step.

6.3 Validation of the model

The validity of the proposed model was evaluated using the oedometer tests of the sand-marine clay mixtures, considering different mass fractions and different initial water contents of the clay matrix. The initial specific volume is adopted as the one in vicinity of the remolded yield stress which is shown in Fig. 16. It increases with both the clay fraction and the initial water content of the clay matrix. The model parameters and initial stress levels for each test are listed in Table 2. The predicted compression curves are shown in Fig. 17 together with the experimental data. It can be seen that there are some differences between the test data and the model predictions at a lower initial water content of the clay matrix (w_c= 67.9 %). However, the compression behavior of the mixtures can be well reproduced by the model for the other three initial water contents. The percolation effect in field projects is significant in case of a high initial water content of the clay matrix. In this case, the overall compression behavior can be well described by the proposed model.

The model was formulated based on the tangent stiffness. The predicted values of the stiffness relationship (between the overall stiffness and the local stiffness) are compared with the experimental data as shown in Fig. 18. The pattern is close to that observed experimentally that the curve with a higher mass fraction lies above the one with a lower fraction. An inconsistency with small values of the stiffness is induced by the remolded yield stress at very low stress levels.

7 Conclusions

In this paper, a series of oedometer tests with different clay mass clay fractions and different initial water contents of the clay matrix was performed on remolded sand-marine clay mixtures. The effect of initial water content on the compression behavior has been discussed, and the evolution of corresponding local variables (e.g., the local specific volume and the local stress of the clay matrix) has been analyzed. Finally, a simple compression model is formulated within homogenization framework. The following conclusions are drawn:

(1) The initial water content of the clay matrix significantly affects the compression behavior of the investigated sand-clay mixtures within the testing stress levels. In this case, the Normal Compression Line of a sand-clay mixture depends on both the mass fraction and the initial water content of the clay matrix.

(2) The local stress in the clay matrix is computed referring to the Normal Compression Line of the pure clay at a specified initial water content. The stress ratio of the mixtures σ'_c/σ', with a sand mass fraction of 20% is approximately close to one. The stress ratio falls significantly with increasing effective overall stress for a sand fraction of 60%, which may be attributed to the formation of clay bridges between adjacent sand particles.

(3) A homogenization equation coupling the overall stiffness E and that of the clay matrix E_c is proposed based on the analysis of the experimental tangent stiffness. A model parameter ξ is introduced considering the sensitivity of the structure parameter on the volume fraction of the clay matrix.

(4) A compression model is formulated based on the tangent stiffness. For a given initial water content of the clay matrix, only three model parameters are included. The model can well predict the compression behavior of the sand-marine clay mixture within the testing stress range.

Limitations of the model are made as follows:

This paper deals with a composite material consisting of sand particles and soft clay matrix within the inter-granular space. Therefore, two limit cases are incorporated: (1) a mixture with negligible fraction of sand, i.e., a pure clay, and (2) a binary mixture with a volume fraction of the clay matrix equaling the minimum inter-lump porosity of the corresponding pure sand material. If the clay fraction is too low to fill the inter-granular space, macro voids between sand particles could exist, and it cannot be modeled by the proposed model.

Acknowledgement

The work in this paper is supported by a National State Key Project "973" grant (Grant No.: 2014CB047000) (sub-project No. 2014CB047001) from Ministry of Science and Technology of the People's Republic of China, a CRF project (Grant No.: PolyU12/CRF/13E) from Research Grants Council (RGC) of Hong Kong Special Administrative Region Government of China. The authors gratefully acknowledge Dr. H. C. Mark Chan and Dr. W. Q. Feng for their comments on the draft manuscript and supports from PolyU Shenzhen Research Institute, and The Hong Kong Polytechnic University, China.

References

Bian, X., Wang, Z. F., Ding, G. Q., & Cao, Y. P. (2016). Compressibility of cemented dredged clay at high water content with super-absorbent polymer. Engineering Geology, 208, 198-205.

Boutin, C., Kacprzak, G., & Thiep, D. (2011). Compressibility and permeability of sand-kaolin mixtures. Experiments versus non-linear homogenization schemes. International Journal for Numerical and Analytical Methods in Geomechanics, 35(1), 21-52.

British Standards Institution (1991). Methods of test for soils for civil engineering purposes, BS 1377. BSI, Milton Keynes.

Burland, J. B. (1990). On the compressibility and shear strength of natural clays. Géotechnique, 40(3), 329-378.

Butterfield, R. (1979). A natural compression law for soils (an advance on *e*-log p'). Géotechnique, 29(4).

Cerato, A. B., & Lutenegger, A. J. (2004). Determining intrinsic compressibility of fine-grained soils. Journal of Geotechnical and Geoenvironmental Engineering, 130(8), 872-877.

Chu, C., Wu, Z., Deng, Y., Chen, Y., & Wang, Q. (2017). Intrinsic Compression Behavior of Remolded Sand-Clay Mixture. Canadian Geotechnical Journal.

Chu, J., & Leong, W. K. (2002). Effect of fines on instability behavior of loose sand. Géotechnique, 52(10), 751-755.

Elkady, T. Y., Shaker, A. A., & Dhowain, A. W. (2015). Shear strengths and volume changes of sand-attapulgite clay mixtures. Bulletin of Engineering Geology and the Environment, 74(2), 595-609.

Fukue, M., Okusa, S., & Nakamura, T. (1986). Consolidation of sand-clay mixtures. In Consolidation of Soils: Testing and Evaluation. ASTM International.

Fukushima, S., & Tatsuoka, F. (1984). Strength and deformation characteristics of saturated sand at extremely low pressures. Soils and Foundations, 24(4), 30-48.

Graham, J., Saadat, F., Gray, M. N., Dixon, D. A., & Zhang, Q. Y. (1989). Strength and volume change behavior of a sand-bentonite mixture. Canadian Geotechnical Journal, 26(2), 292-305.

Hashiguchi, K. (1995). On the linear relations of *v*-ln*p* and ln*v*-ln*p* for isotropic consolidation of soils. International journal for numerical and analytical methods in geomechanics, 19(5), 367-376.

Hashin, Z. (1983). Analysis of composite materials. J. appl. Mech, 50(2), 481-505.

Herle, I., & Gudehus, G. (1999). Determination of parameters of a hypoplastic constitutive model from properties of grain assemblies. Mechanics of Cohesive-frictional Materials, 4(5), 461-486.

Hong, Z. (2007). Void Ratio-Suction Behavior of Remolded Ariake Clays. Geotechnical Testing Journal 30(3), 234-239.

Hong, Z., & Onitsuka, K. (1998). A method of correcting yield stress and compression index of Ariake clays for sample disturbance. Soils and foundations, 38(2), 211-222.

Hong, Z., Yin, J., & Cui, Y. J. (2010). Compression behavior of reconstituted soils at high initial water contents. Géotechnique, 60(9), 691-700.

Hong, Z. S., Zeng, L. L., Cui, Y. J., Cai, Y. Q., & Lin, C. (2012). Compression behavior of natural and reconstituted clays. Ge̒otechnique, 62(4), 291.

Horpibulsuk, S., Liu, M. D., Zhuang, Z., & Hong, Z. S. (2016). Complete compression curves of reconstituted clays. International Journal of Geomechanics, 16(6).

Jafari, M. K., & Shafiee, A. (2004). Mechanical behavior of compacted composite clays. Canadian Geotechnical Journal, 41(6), 1152-1167.

Karunaratne, G. P., Yong, K. Y., Tan, T. S., Tan, S. A., Liang, K. M., Lee, S. L., & Vijiaratnam, A. (1990, April). Layered clay-sand scheme reclamation at Changi South Bay. In Proc. 10th Southeast Asian Geotech. Conf., Southeast Asian Society of Soil Mechanics and Found. Engrg (pp. 71-76).

Karunaratne, G. P., Yong, K. Y., Tan, T. S., Tan, S. A., Lee, S. L., & Vijiaratnam, A. (1991). Land reclamation using layered clay-sand scheme. Proceedings GEO-COAST, 91, 335-340.

Kumar, G. V. (1996). Some aspects of the mechanical behavior of mixtures of kaolin and coarse sand (Doctoral dissertation, University of Glasgow).

Kumar, G. V., & Wood, D. M. (1999). Fall cone and compression tests on clay-gravel mixtures. Ge̒otechnique, 49(6), 727-739.

Liu M. D., Carter J. P. and Airey D. W. (2011). Sydney Soil model: (I) theoretical formulation, International Journal of Geomechanics, ASCE, 11(3), 211-224.

Liu, M. D., Zhuang, Z., & Horpibulsuk, S. (2013). Estimation of the compression behavior of reconstituted clays. Engineering Geology, 167, 84-94.

Martins, F. B., Bressani, L. A., Coop, M. R., & Bica, A. V. D. (2001). Some aspects of the compressibility behavior of a clayey sand. Canadian Geotechnical Journal, 38(6), 1177-1186.

Mesri, G., & Vardhanabhuti, B. (2009). Compression of granular materials. Canadian Geotechnical Journal, 46(4), 369-392.

Mitchell, J. K. 1993, Fundamentals of Soil Behavior, John Wiley and Sons, Inc., New York.

Monkul, M. M., & Ozden, G. (2005). Effect of intergranular void ratio on one-dimensional compression behavior. In Proceedings of International Conference on Problematic Soils, Inter- national Society of Soil Mechanics and Geotechnical Engineering, Famagusta, Turkish Republic of Northern Cyprus (Vol. 3, pp. 1203-1209).

Monkul, M. M., & Önal, O. (2006). A visual basic program for analyzing oedometer test results and evaluating intergranular void ratio. Computers & geosciences, 32(5), 696-703.

Monkul, M. M., & Ozden, G. (2007). Compressional behavior of clayey sand and transition fines content. Engineering Geology, 89(3), 195-205.

Pestana J. M. and Whittle A. J. (1995). Compression model for cohesionless soils, Géotechnique, 45(4), 621-631.

Pitman, T. D., Robertson, P. K., & Sego, D. C. (1994). Influence of fines on the collapse of loose sands. Canadian Geotechnical Journal, 31(5), 728-739.

Saada, A., & Puccini, P. (1988). The development of a data base using the Case hollow cylinder apparatus. Constitutive equations for granular non-cohesive, 33-40.

Shi, X. S., & Herle, I. (2015). Compression and undrained shear strength of remoulded clay mixtures. Géotechnique Letters, 5(2), 62-67.

Shi, X. S. and Herle, I. (2016a). Numerical simulation of lumpy soils using a hypoplastic model. Acta Geotechnica 11.

Shi, X. S., & Herle, I. (2016b). Modeling the compression behavior of remolded clay mixtures. Computers and Geotechnics, 80, 215-225.

Silva, S. D. Three runway system project (3RS project), contract 3206 - main reclamation works. Report for ZHECC-CCCC-CDC joint venture. 7076481/R00: Hong Kong, 2016.

Sridharan, A. & Prakash, K. (1996). Discussion on 'interpretation of oedometer test data for natural clays.' Soils and Foundations 36(3), 146-148.

Tan, S. A., Karunaratne, G. P., & Muhammad, N. (1994). Sand penetration into clay slurry through jute interlayer. Soils and foundations, 34(2), 19-25.

Tsuchida, T. (2017). e-log σ_V relationship for marine clays considering initial water content to evaluate soil structure. Marine Georesources & Geotechnology, 35(1), 104-119.

Tu, S. T., Cai, W. Z., Yin, Y., & Ling, X. (2005). Numerical simulation of saturation behavior of physical properties in composites with randomly distributed second-phase. Journal of composite materials, 39(7), 617-631.

Weng, G. J., & Tandon, G. P. (1988). A theory of particle-reinforced plasticity. ASME Journal of Applied Mechanics, 55(3), 126-135.

Yin, J. H. (1999). Properties and behavior of Hong Kong marine deposits with different clay contents. Canadian Geotechnical Journal, 36(6), 1085-1095.

Zeng, L. L., Hong, Z. S., & Cui, Y. J. (2015). Determining the virgin compression lines of reconstituted clays at different initial water contents. Canadian Geotechnical Journal, 52(9), 1408-1415.

Zeng L L, Hong Z S, Cui Y J. (2016a) Time-dependent compression behaviour of dredged clays at high water contents in China. Applied Clay Science, 123: 320-328.

Zeng, L. L., Hong, Z. S., & Gao, Y. F. (2016b). Practical estimation of compression behaviour of dredged clays with three physical parameters. Engineering Geology.

List of Tables

Table 1: Basic physical properties of the tested materials

Materials	Density of particles	Liquid limit	Plastic limit	Clay	Silt	Sand
—	(Mg/m^3)	(%)	(%)	(%)	(%)	(%)
Clay	2.68	62.4	27.5	15	85	0
Sand	2.63	—	—	0	0	100

Table 2: Parameters of the proposed compression model for the sand-marine clay mixtures

Specimens	w_{c0} (%)	N_c	λ_c	Sand fraction ϕ_c (%)	ξ	Initial stress level (kPa)
Series-1	67.9	1.121	0.083	100, 80, 60, 40	0.75	5.0
Series-2	74.5	1.156	0.087	100, 80, 60, 40	0.75	2.5
Series-3	86.9	1.238	0.100	100, 80, 60, 40	0.75	1.7
Series-4	99.5	1.296	0.102	100, 80, 60, 40	0.75	1.7

List of Figures

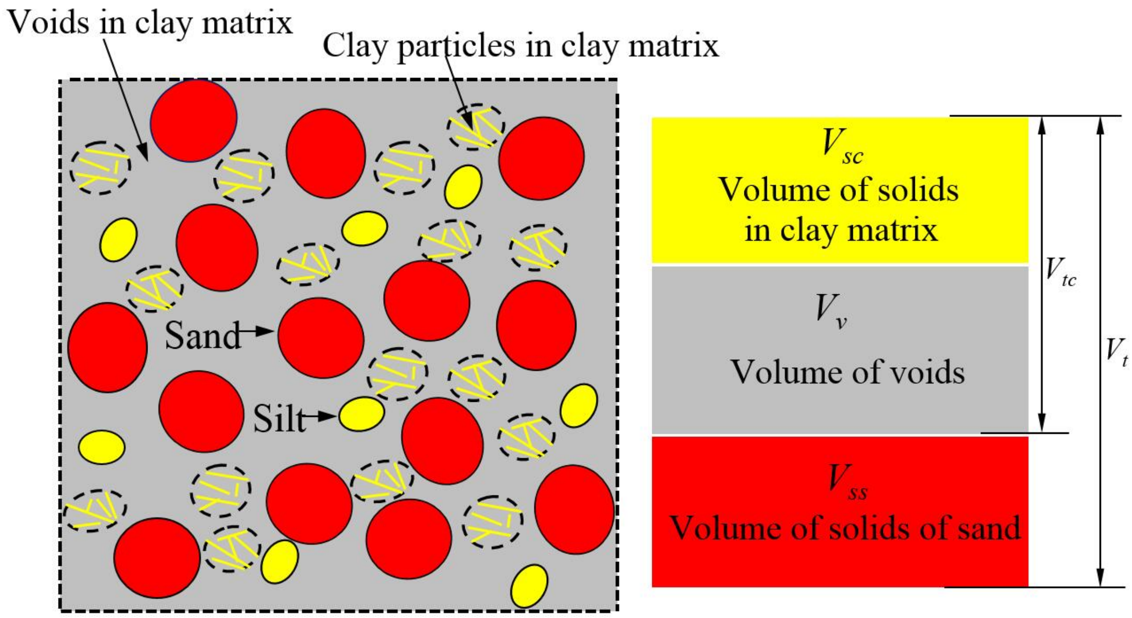

Figure 1: Divisions of the volumes in sand-clay mixture

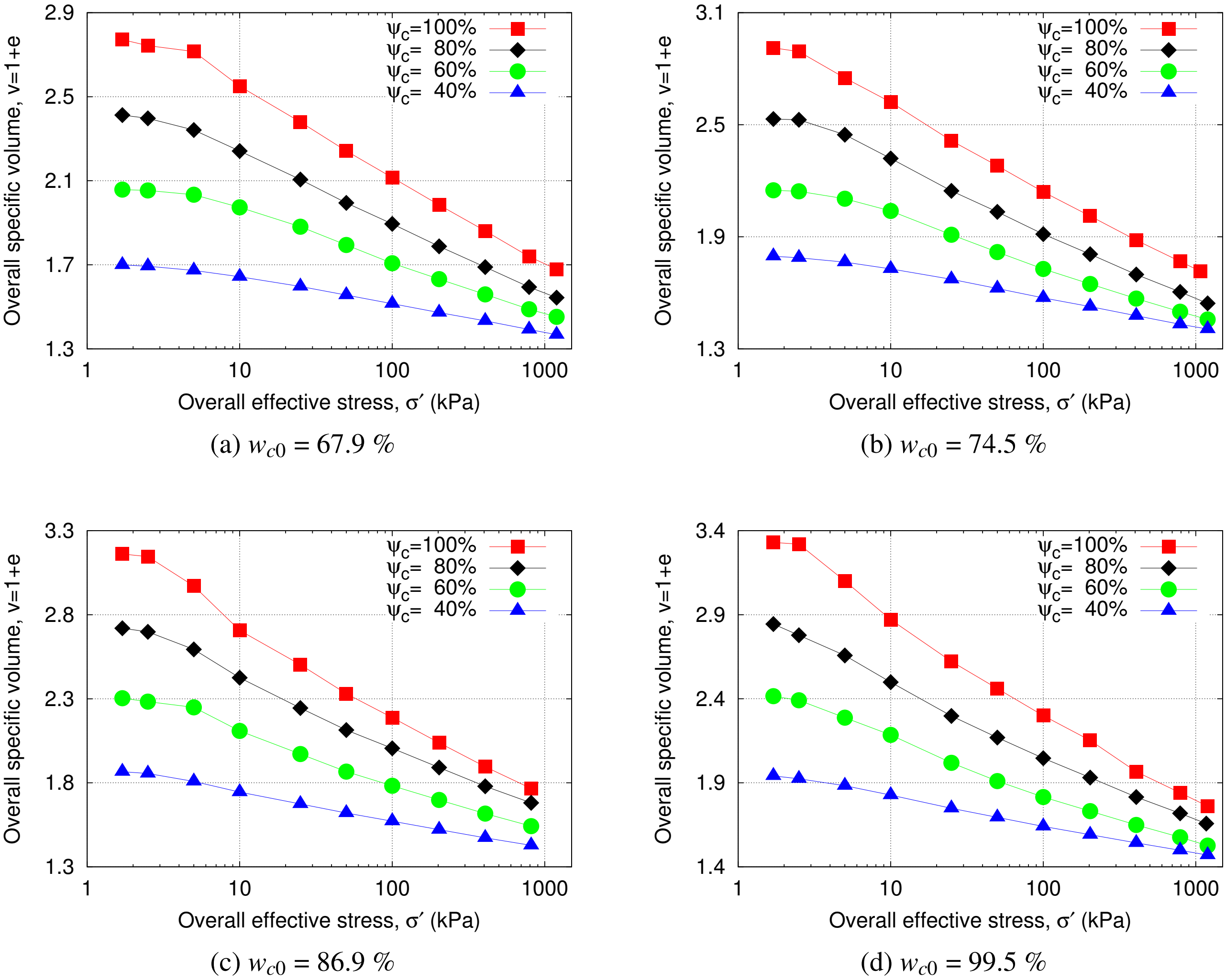

(a) w_{c0} = 67.9 %

(b) w_{c0} = 74.5 %

(c) w_{c0} = 86.9 %

(d) w_{c0} = 99.5 %

Figure 2: Compression curves of sand-clay mixtures with different mass fractions of the clay matrix

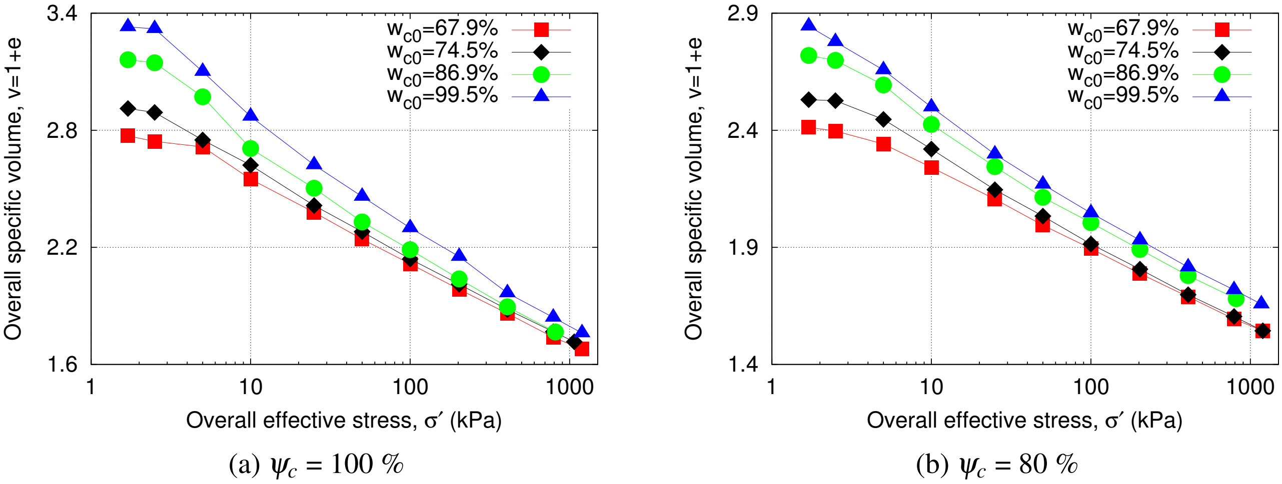

(a) ψ_c = 100 %

(b) ψ_c = 80 %

(c) ψ_c = 60 %

(d) ψ_c = 40 %

Figure 3: Compression curves of sand-clay mixtures at different initial water contents of the clay matrix

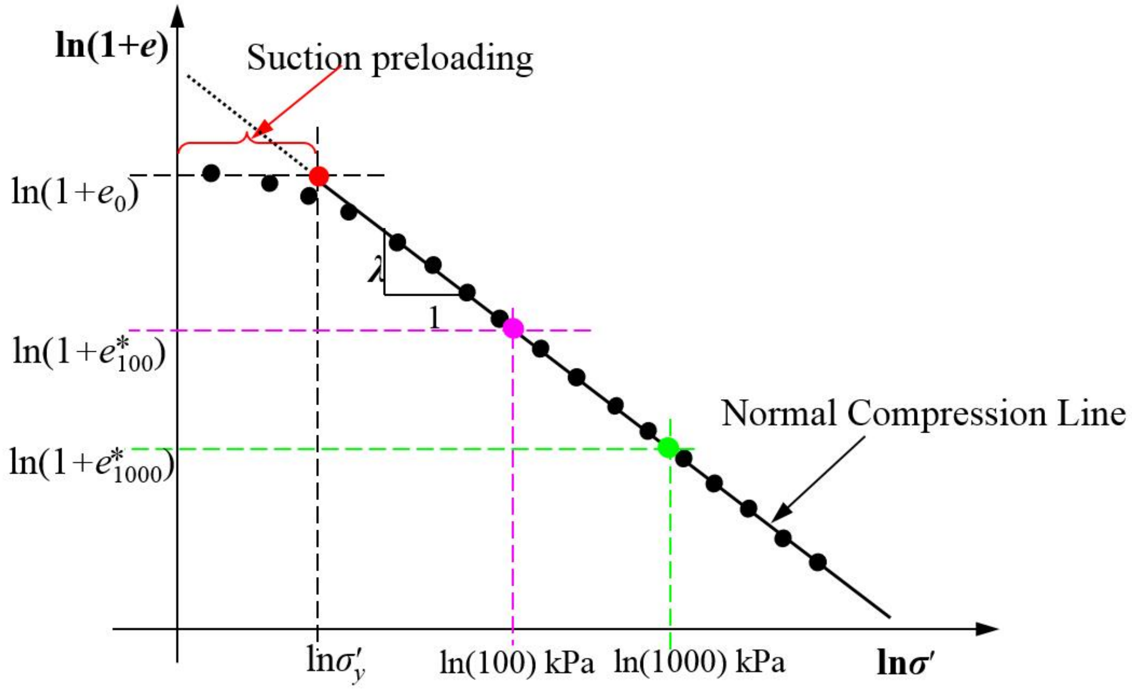

Figure 4: Schematic plot for the interpretation of the compression behaviour of remolded sand-clay mixtures

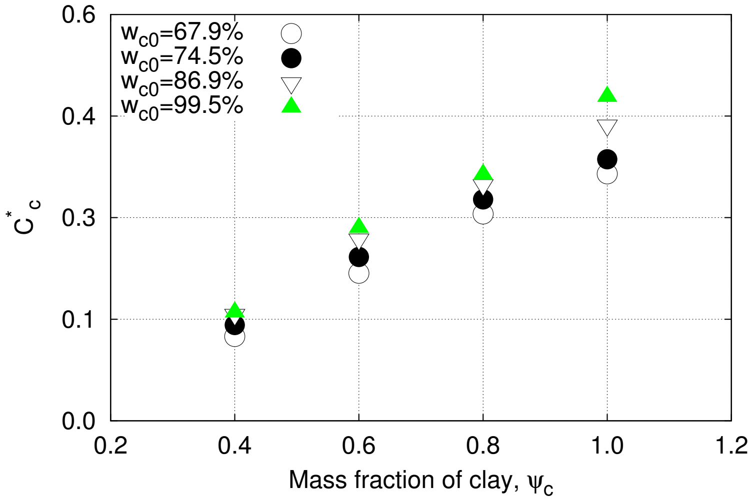

(a) C_c^*

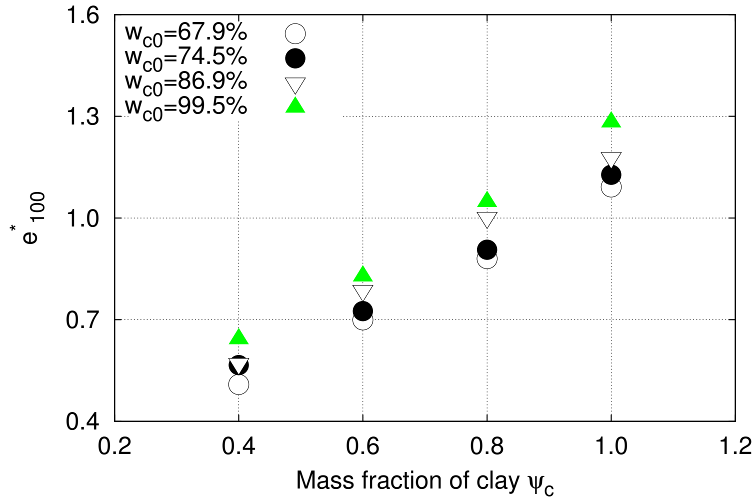

(b) e_{100}^*

Figure 5: Change of the intrinsic compression parameters with mass fraction of the clay matrix

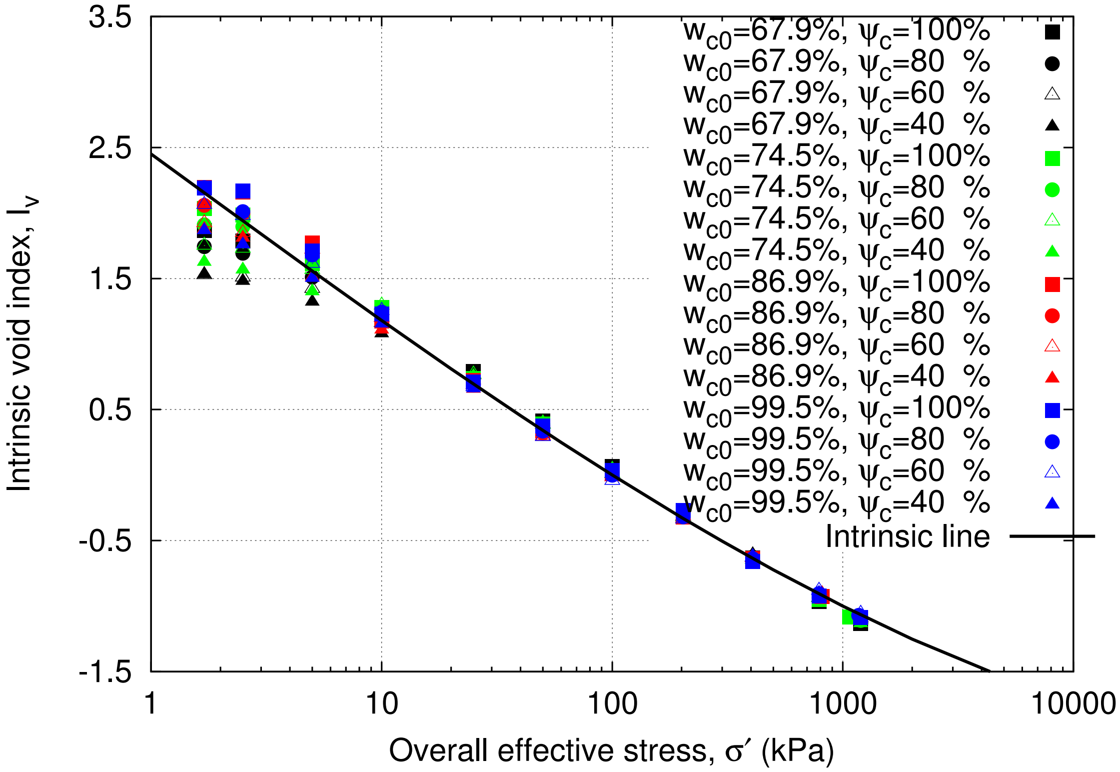

Figure 6: Intrinsic compression curves of the sand-clay mixtures with different mass fractions and different initial water contents

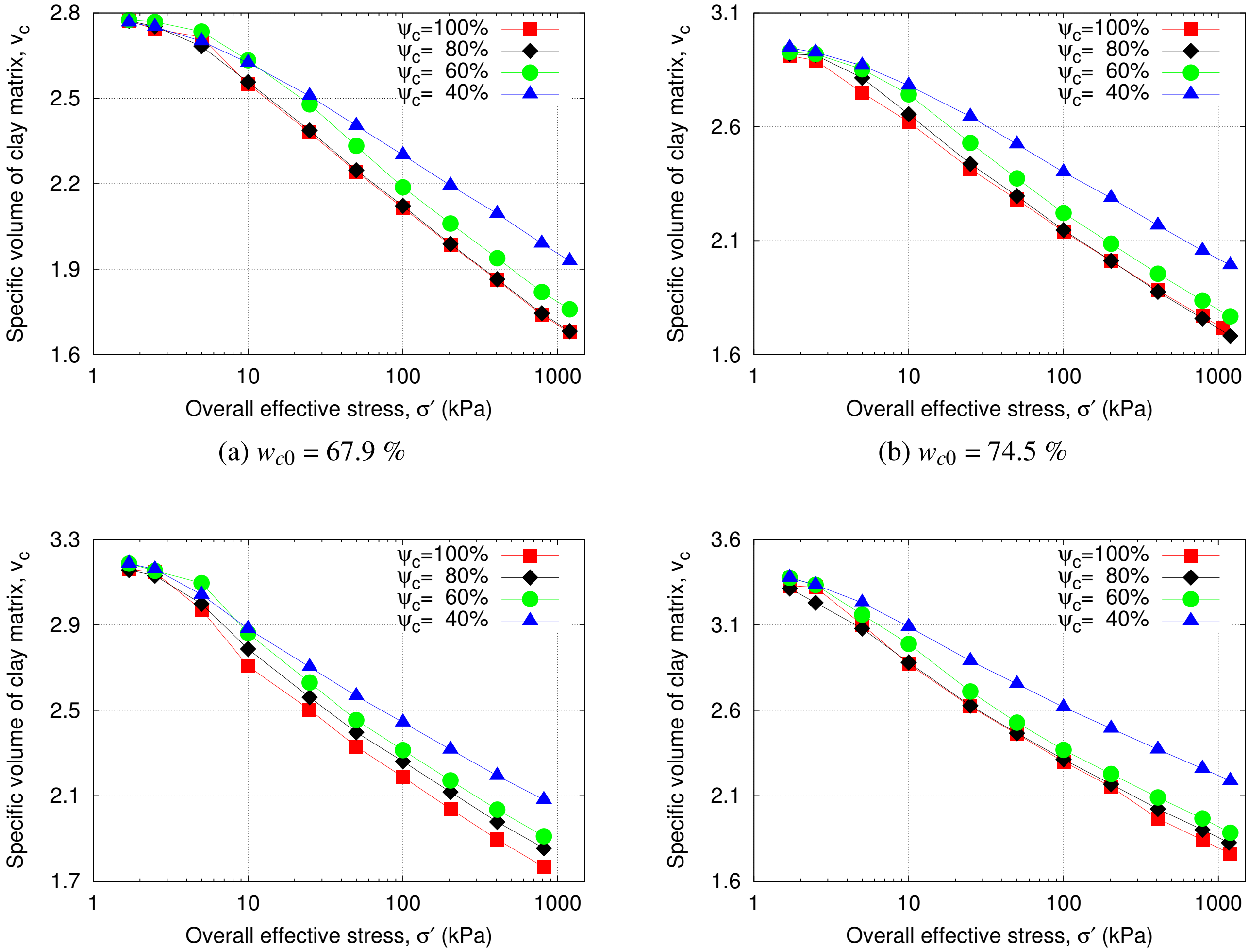

(a) w_{c0} = 67.9 %

(b) w_{c0} = 74.5 %

(c) w_{c0} = 86.9 %

(d) w_{c0} = 99.5 %

Figure 7: Compression curves of the clay matrix in sand-clay mixtures with different mass fractions of clay matrix

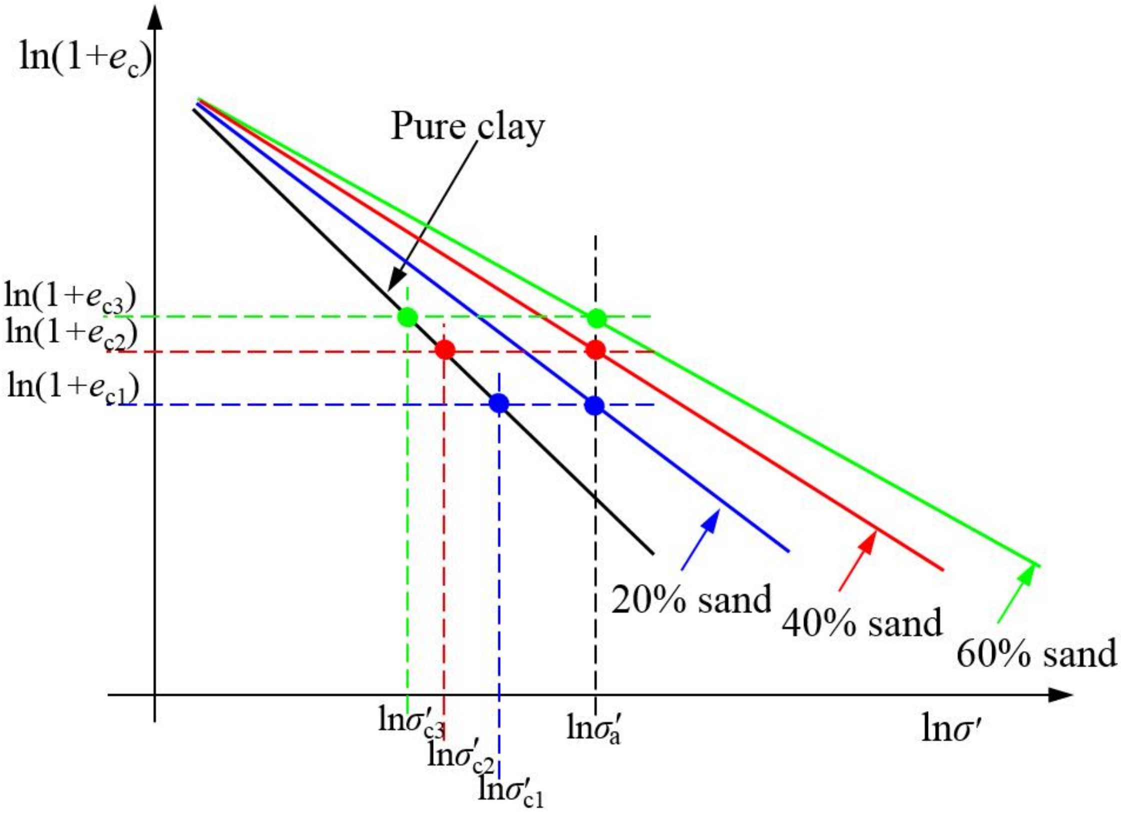

Figure 8: Schematic plot for the calculation of the local stress in remolded sand-clay mixtures

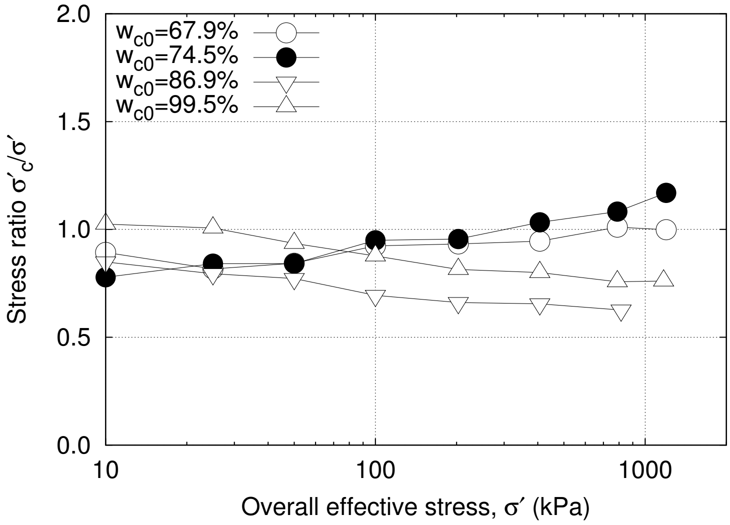

(a) ψ_c = 80 %

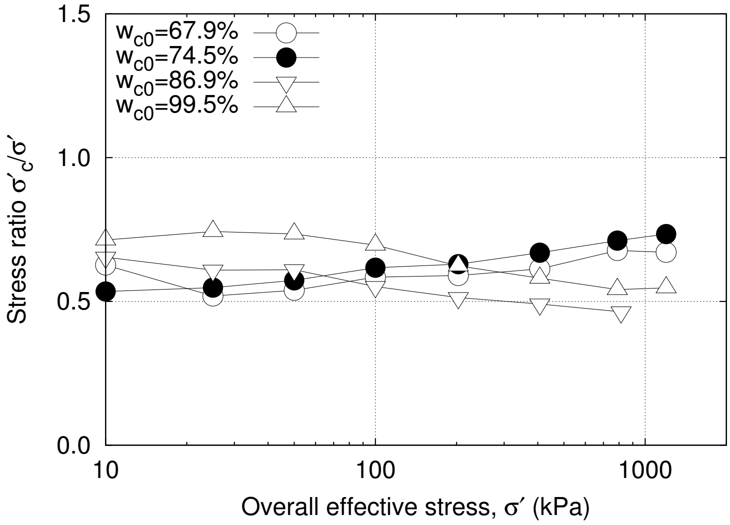

(b) ψ_c = 60 %

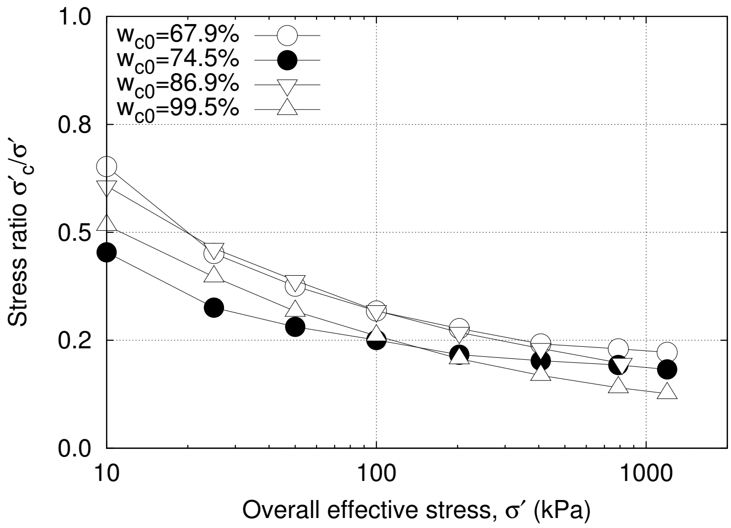

(c) ψ_c = 40 %

Figure 9: Stress ratio between the clay matrix and the sand-clay mixtures

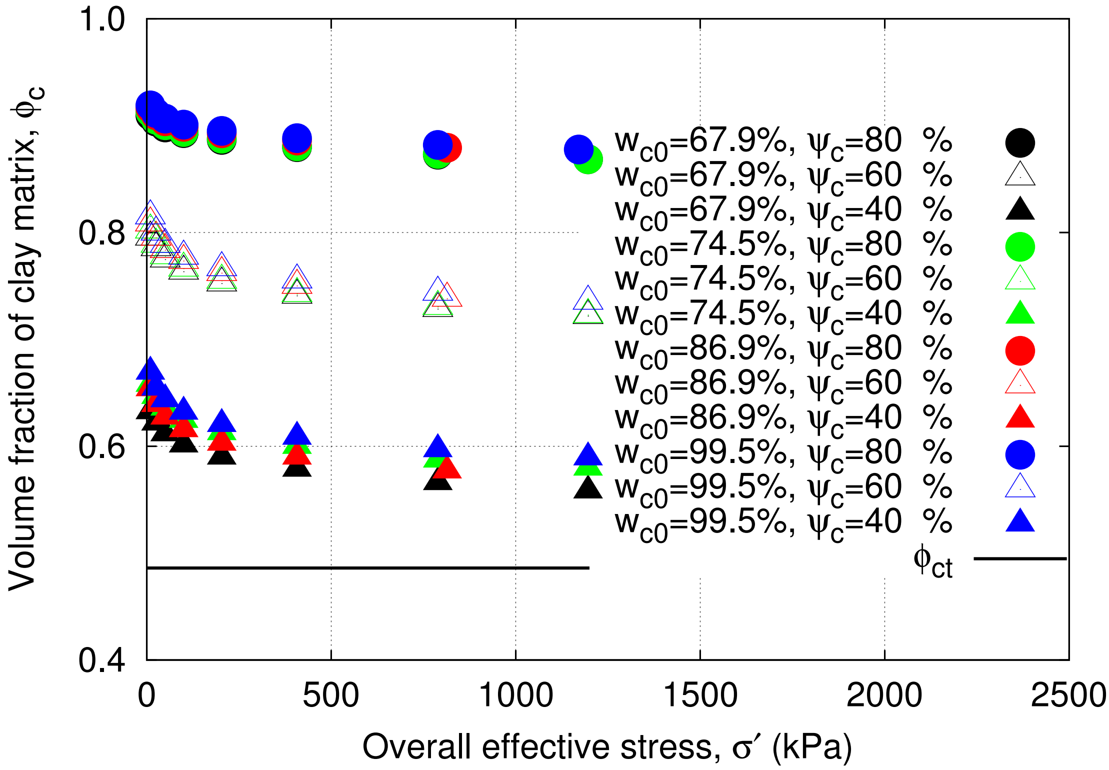

Figure 10: Evolution of the volume fraction of the clay matrix in remolded sand-clay mixtures

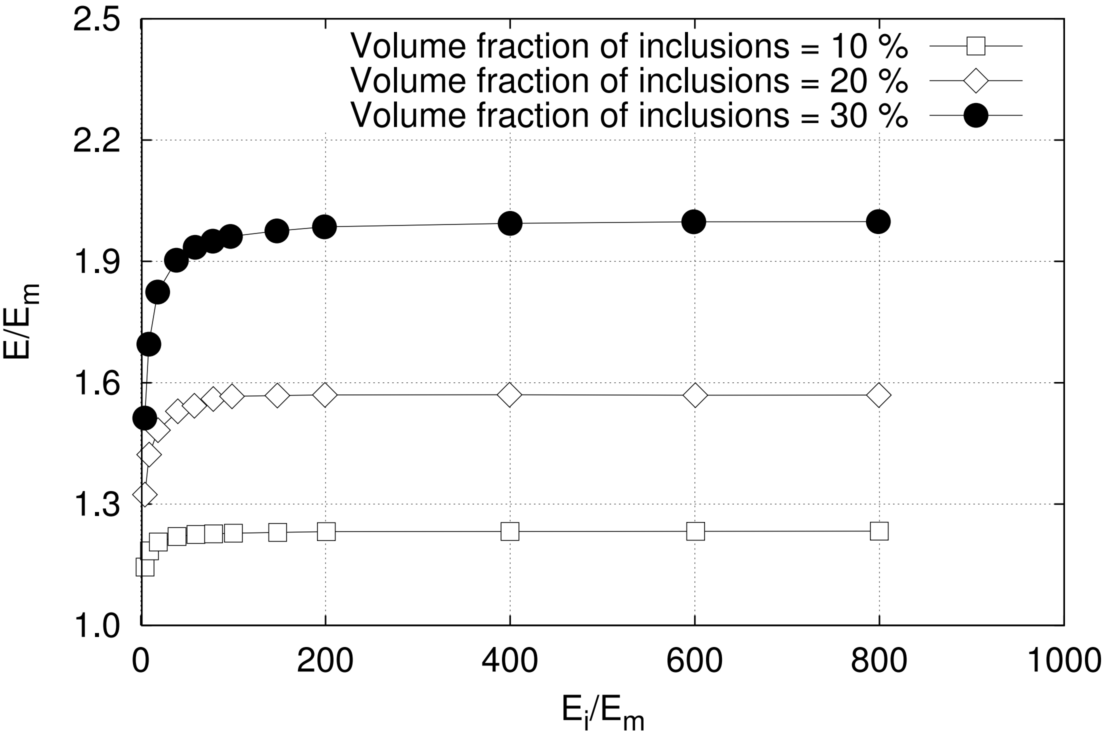

Figure 11: Evolution of the overall elastic stiffness with increasing elastic stiffness of the inclusions (Tu *et al.*, 2005)

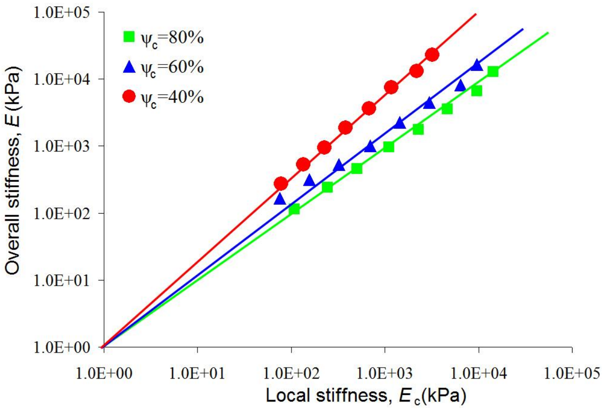

(a) w_{c0} = 67.9 %

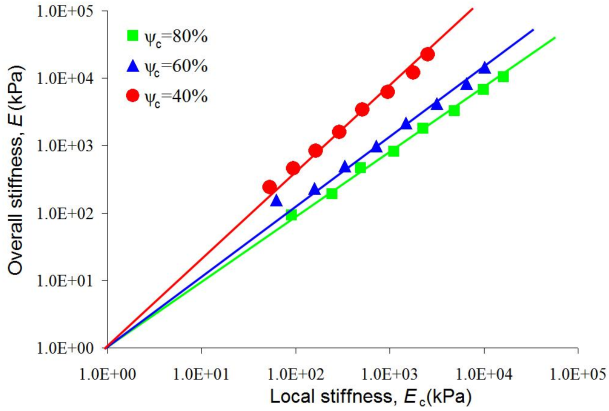

(b) w_{c0} = 74.5 %

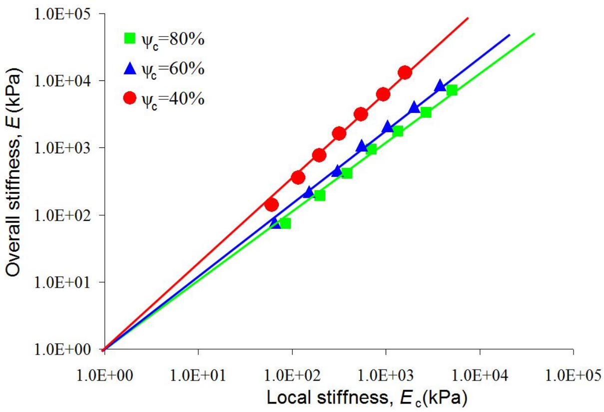

(c) w_{c0} = 86.9 %

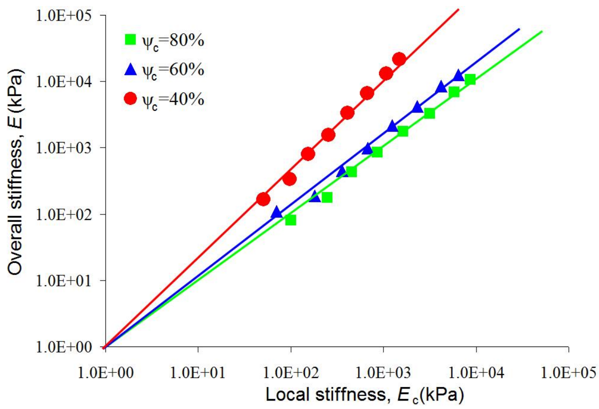

(d) w_{c0} = 99.5 %

Figure 12: Stiffness relationship between the clay matrix and the sand-clay mixtures

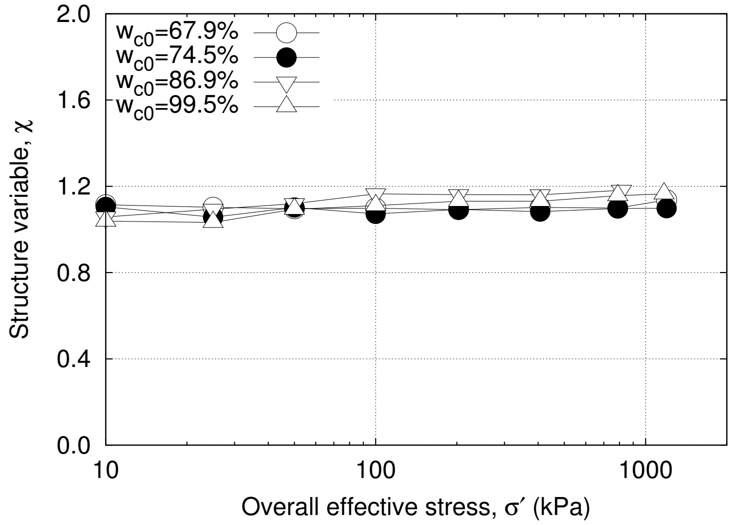

(a) ψ_c = 80 %

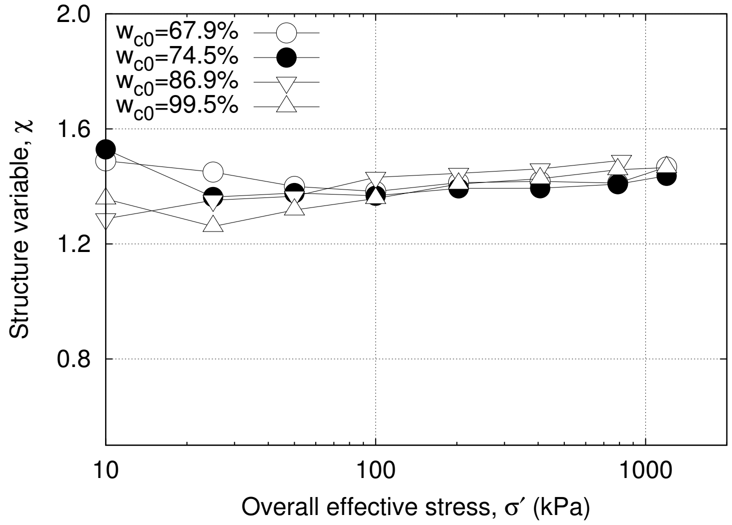

(b) ψ_c = 60 %

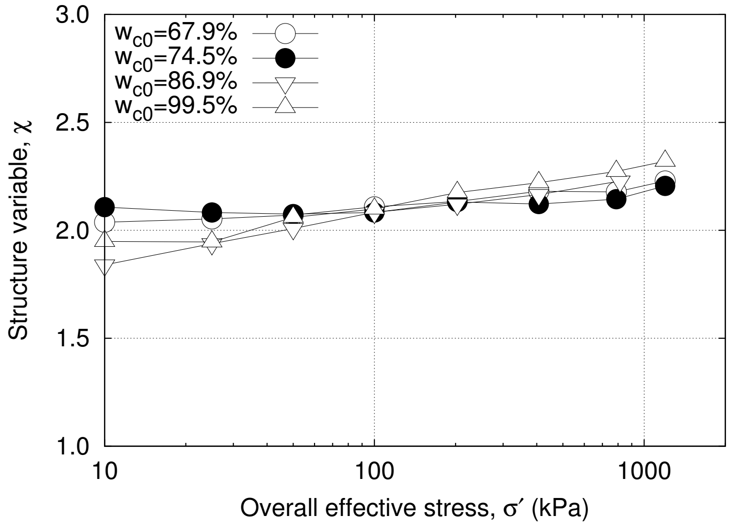

(c) ψ_c = 40 %

Figure 13: Relationship between the structure variable χ and effective stress level

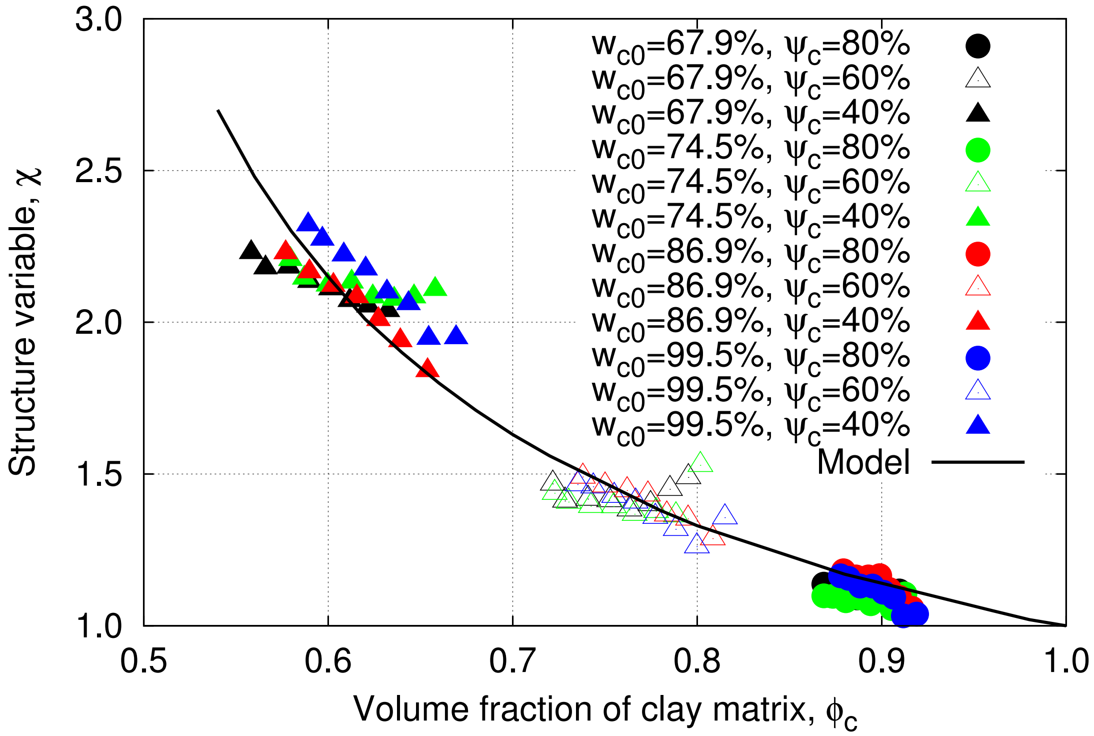

Figure 14: Relationship between the structure parameter and the volume fraction of the clay matrix

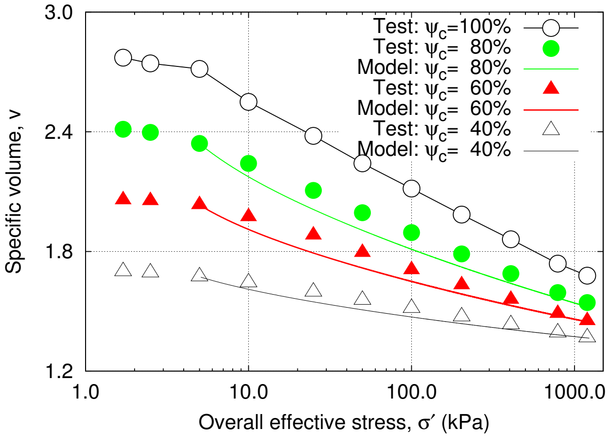

(a) w_{c0} = 67.9 %

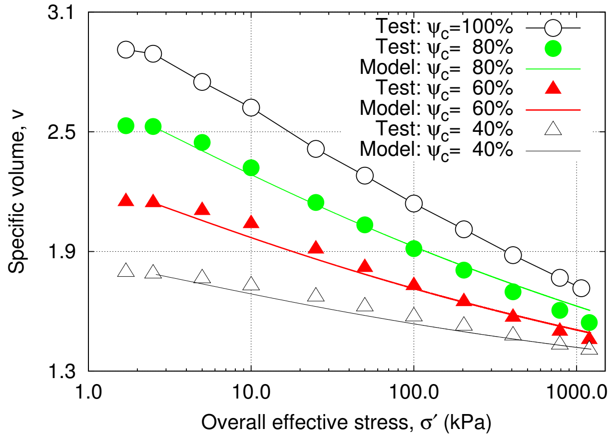

(b) w_{c0} = 74.5 %

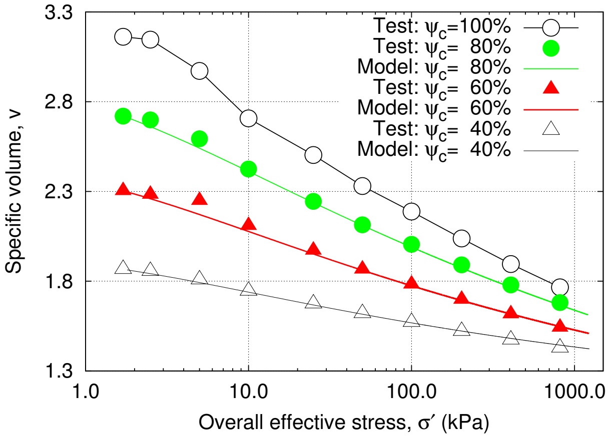

(c) w_{c0} = 86.9 %

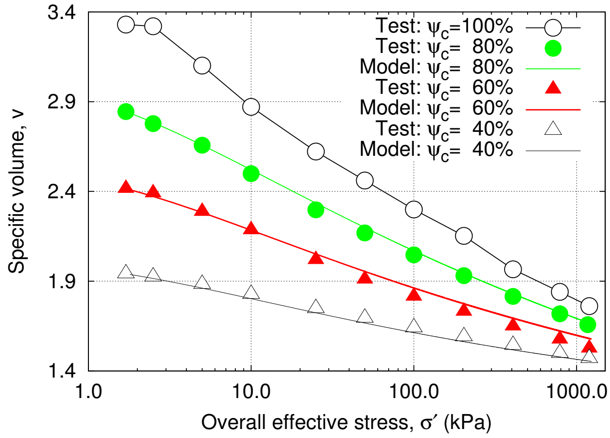

(d) w_{c0} = 99.5 %

Figure 15: Comparison between the predicted compression curves and the experimental data

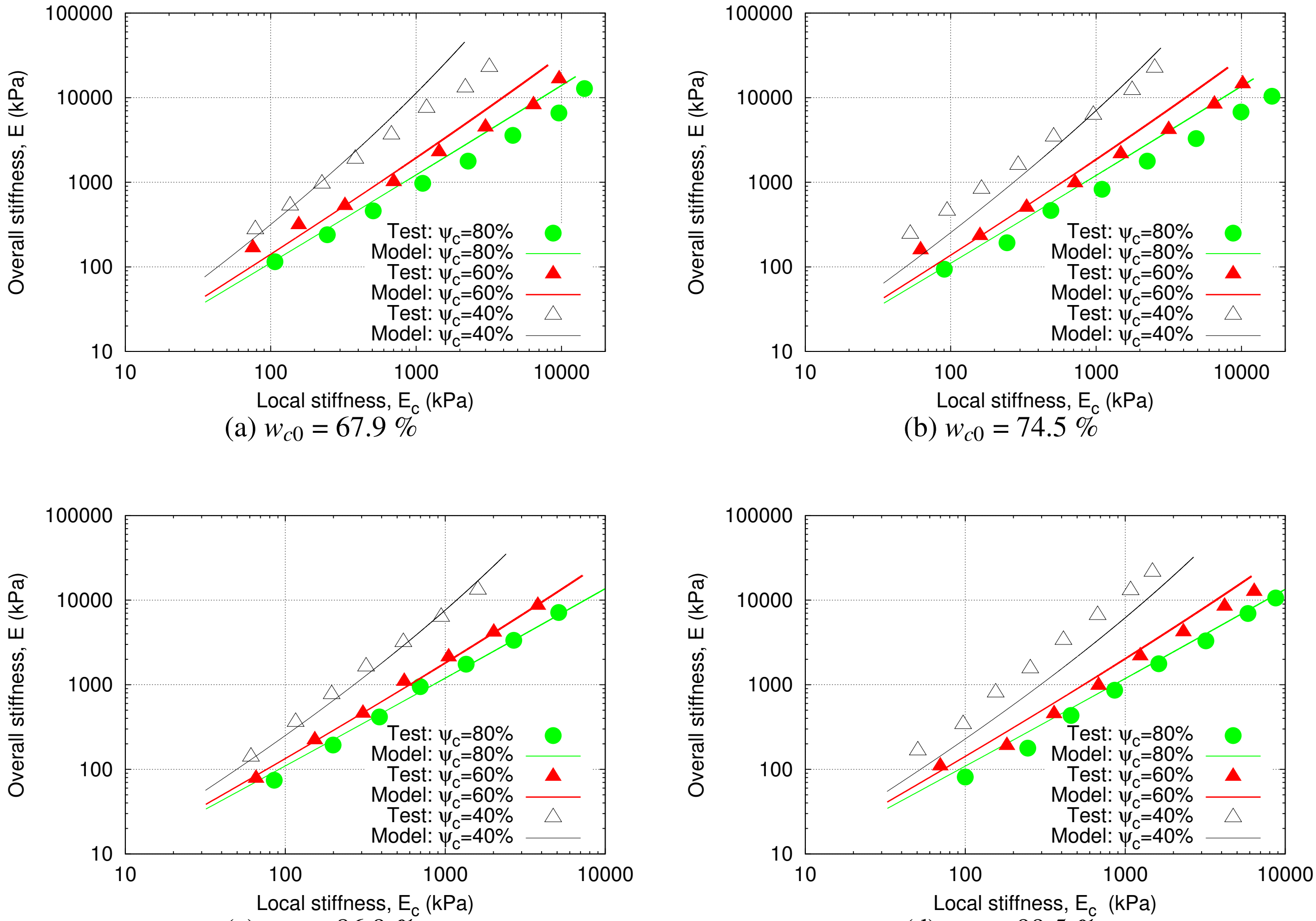

(a) $w_{c0} = 67.9$ %

(b) $w_{c0} = 74.5$ %

(c) $w_{c0} = 86.9$ %

(d) $w_{c0} = 99.5$ %

Figure 16: Prediction of the relationship between the local stiffness and the overall stiffness